



HAL
open science

Under Glass Weathering of Hemp Fibers Reinforced Polypropylene Biocomposites: Degradation Mechanisms Based on Emitted Volatile Organic Compounds

Célia Badji, Jean-Marc Sotiropoulos, J. Beigbeder, Hélène Garay, Anne Bergeret, J-C Bénézet, V. Desauziers

► To cite this version:

Célia Badji, Jean-Marc Sotiropoulos, J. Beigbeder, Hélène Garay, Anne Bergeret, et al.. Under Glass Weathering of Hemp Fibers Reinforced Polypropylene Biocomposites: Degradation Mechanisms Based on Emitted Volatile Organic Compounds. *Frontiers in Materials*, 2020, 7, 10.3389/fmats.2020.00162 . hal-02873563

HAL Id: hal-02873563

<https://imt-mines-ales.hal.science/hal-02873563>

Submitted on 18 Jun 2020

HAL is a multi-disciplinary open access archive for the deposit and dissemination of scientific research documents, whether they are published or not. The documents may come from teaching and research institutions in France or abroad, or from public or private research centers.

L'archive ouverte pluridisciplinaire **HAL**, est destinée au dépôt et à la diffusion de documents scientifiques de niveau recherche, publiés ou non, émanant des établissements d'enseignement et de recherche français ou étrangers, des laboratoires publics ou privés.



Under Glass Weathering of Hemp Fibers Reinforced Polypropylene Biocomposites: Degradation Mechanisms Based on Emitted Volatile Organic Compounds

Célia Badji^{1,2}, Jean-Marc Sotiropoulos³, Joana Beigbeder¹, Hélène Garay¹, Anne Bergeret², Jean-Charles Bénézet² and Valérie Desauziers^{1*}

¹ IPREM, IMT Mines Ales, Université de Pau et des Pays de l'Adour, E2S UPPA, CNRS, Pau, France, ² IPREM, Université de Pau et des Pays de l'Adour, E2S UPPA, CNRS, Pau, France, ³ PCH, IMT Mines Ales, Ales, France

OPEN ACCESS

Edited by:

Patricia Krawczak,
IMT Lille Douai, France

Reviewed by:

Xavier Colin,
École Nationale Supérieure d'Arts et
Métiers, ParisTech, France

Dan Maskell,
University of Bath, United Kingdom

Asim Shahzad,
National University of Sciences
and Technology (NUST), Pakistan

*Correspondence:

Valérie Desauziers
Valerie.Desauziers@mines-ales.fr

Specialty section:

This article was submitted to
Polymeric and Composite Materials,
a section of the journal
Frontiers in Materials

Received: 09 March 2020

Accepted: 04 May 2020

Published: 18 June 2020

Citation:

Badji C, Sotiropoulos J-M,
Beigbeder J, Garay H, Bergeret A,
Bénézet J-C and Desauziers V (2020)
Under Glass Weathering of Hemp
Fibers Reinforced Polypropylene
Biocomposites: Degradation
Mechanisms Based on Emitted
Volatile Organic Compounds.
Front. Mater. 7:162.
doi: 10.3389/fmats.2020.00162

The durability of hemp fibers reinforced polypropylene biocomposites was investigated after one year under glass exposure. Volatile organic compounds emissions were assessed using a new passive sampling method. Degradation pathways were examined in order to understand the weathering mechanisms. The polymer matrix was decomposed into oxygenated products due to UV rays and high temperatures. As regards hemp fibers, different degradation steps of the carbohydrates were highlighted according to the nature of the detected furans. At a non-weathered state, dehydrations preceded the ring-opening mechanism, often catalyzed by Maillard reactions. The further cyclization induced the formation of 2- or 5-substituted furans emitted by non-weathered materials. Reactions between identified products after weathering which were not yet found in literature were proposed in this paper. They often implied a keto-enol tautomerism but also dehydrations that induced the formation of 3- and 4-substituted furanones. These differences can be explained by a primary decomposition of carbohydrates favored at a non-weathered state and a secondary one occurring at a weathered state.

Keywords: hemp fiber, ageing, VOCs, oxidation, dehydration

INTRODUCTION

Recently, bio-fillers have emerged as an attractive alternative to inorganic fillers in the reinforcement of thermoplastics in response to growing awareness of environmental issues and increasing global waste problems (Liu and Hu, 2008). The main application areas of vegetal filler reinforced composites are the automotive and building industries (John and Thomas, 2008; Azwa et al., 2013). The natural fibers improve the mechanical properties of the composites (Saba et al., 2016; Kumre et al., 2017). Recently, lignin in a lignin-polyethylene (PE) biocomposite showed some antioxidant properties that protect the PE matrix (Van Schoors et al., 2018). Otherwise, with increasing concerns about indoor air quality, volatile organic compounds (VOCs) emissions

behavior in interior materials used as automotive parts has become widely recognized as an important topic for indoor environment air quality (Yu and Crump, 1998; Air quality sciences Inc., 2006; Badji et al., 2018).

During the melt mixing process of biocomposites through extrusion and injection molding, the high manufacturing temperatures exceed the bio-fillers degradation temperature (Dorez et al., 2013; Khazaeian et al., 2015). Also, during their use, climatic conditions weaken their chemical stability because of their high sensitivity (Zou et al., 2008; Ahmad et al., 2011; Badji et al., 2017). Temperature variations induce carbonization and odors emanating from the heated matter. Also, a press molding temperature increase induces biocomposites color turning from brown to close to black (Shibata, 2016). This was thought to be the result of vegetal fibers caramelization. Some solutions for reducing the odors and the amount of VOCs produced by biocomposites have been studied (Kim et al., 2006, 2011). But molecules responsible for the worsening air quality, color changes, and odors must be assessed.

Volatile organic compounds emitted by plastics are generally due to polymer degradation. Studies on thermal and photochemical oxidation of polypropylene (PP) showed that radical processes are responsible for chain scission, leading to low molecular weight products migrating from the polymeric matrix to the atmosphere (François-Heude et al., 2014; Rouillon et al., 2016). It is widely accepted that Norrish type I and II photochemical reactions occur involving C–C cleavage, leading to the formation of oxygenated compounds (Rabek, 1990; Muasher and Sain, 2006). Those generally result from the oxidation of tertiary carbon atoms of the polymer chains, leading to methyl ketones, along with alcohols, aldehydes, and aliphatic hydrocarbons formation.

The pyrolysis of lignocellulosic biomass was widely studied and further identification of the volatile compounds issued from the natural fibers' thermal degradation was sometimes performed. Some products, originating from pyrolysis of cellulose [molecular formula: $(C_6H_{10}O_5)_n$], are identified as low molecular weight compounds. They are formed by ring-opening reactions, while pyrans and furans are obtained from dehydration reactions (Sanders et al., 2003; Nowakowski and Jones, 2008). These molecules are generally stable aromatic compounds and hardly decompose into lower molecular weight compounds (Katō and Komorita, 1968). Their decomposition accounts for the major reactions occurring in the secondary reaction stage of cellulose. Hemicelluloses consist of saccharides such as glucose, mannose, xylose, and arabinose (Nowakowski and Jones, 2008; Binder et al., 2010). Once pyrolyzed, the derivatives of these pentose sugars, such as cyclopentanes and cyclopentenones, are detected in large quantities in addition to furan molecules (Peng and Wu, 2011; Carrier et al., 2012). Lignin component, a highly complex aromatic structure, breaks down into phenolic structures (Wittkowski et al., 1992; Brzonova et al., 2014). It mainly consists of three basic building blocks: guaiacyl, syringyl, and *p*-hydroxyphenyl units. However, non-cellulosic polysaccharides, such as proteins, are also found in lower proportions under amino acid forms (Sari, 2015). Each

component proportion present in the vegetal fibers depends on several parameters such as their nature, retting time, and geographic origin.

Maillard reactions are mainly responsible for the formation of flavor compounds like the 2-furanones with similar structures, unlike those of volatile substances issued from biofillers degradation. Besides the flavoring of food, the interest in Maillard mechanism has grown in fields concerned with the physico-chemical properties of proteins and polysaccharides (Mitsuo, 1988; He et al., 2014). This reaction implies the interaction between the amino group from an amino acid, a protein, or an amine and the carbonyl functional group from the carbohydrate part (glucose, fructose) under heating conditions (Zhang et al., 2008). It produces an unstable N-substituted glycosylamino compound. This first step is reversible but the generated glycosylamine is immediately converted into an Amadori compound (Newton et al., 2012). Amadori intermediate compounds belonging to the 1-amino-1-deoxy-2-ketoses family are important precursors in the formation of flavor compounds from Maillard reactions (Hodge et al., 1972; Zhang et al., 2008). Caramelized sugar aromas furanones, such as furfural and 5-methylfurfural, or pyranones such as maltol, evolving from holocellulose, are generated through sugar-amine condensation. Then, the formed Amadori compound can react along multiple pathways to form Maillard reaction products at lower temperatures than those found in pyrolysis studies of natural fibers, since the presence of nitrogen containing compounds catalyzes the reaction (Newton et al., 2012). For instance, maltol, a well-known carbohydrate derivative, and 4-hydroxy-2,5-dimethyl-3(2H)-furanone, derives from a common intermediate arising by sugar-amine condensation and Amadori rearrangement. 2,3-enolization of the 1-amino-1-deoxy-2-ketose and elimination of the 1-amino group occur at the final step (Hodge et al., 1972). Then, dehydrations and cyclization lead to furans generation (Wang et al., 2012) and ene-diol scissions and retroaldolization to short products (Belitz et al., 2004).

However, formations of the substances found in literature dealing with biomass and their controlled decomposition (pyrolysis) were not explained to be due to this mechanism. Indeed, the reactions involved require the presence of artificial catalysts (chromium, copper) facilitating the conversion (Binder et al., 2010; Perez and Fraga, 2014). Otherwise, when decomposition products are obtained from the pyrolysis process, this includes energetic conditions favorable enough (temperature reaching 800°C) that ring-opening, dehydrogenation, and cracking can occur (Sanders et al., 2003; Peng and Wu, 2011). Moreover, formation of other methylfurans that could issue from thermal decomposition and reactions between volatile chemicals emitted by natural fibers were not reported.

A one-year natural under-glass weathering of hemp fibers reinforced PP biocomposites was investigated to simulate a car interior environment. Volatile organic compounds emissions were assessed throughout the process. The objective was to use the identification of emitted VOCs to understand the components' method of degradation by firstly studying the neat polymer ageing and secondly the aging of the hemp fibers load

in the polymer matrix. The well-known Maillard mechanism for the holocellulose part decomposition has been examined thanks to VOCs identification. Reactions between identified VOCs and their concentration evolution were proposed. Finally, the lignin degradation was also investigated.

MATERIALS AND METHODS

Materials

Polypropylene grade H733-07 with a melt flow rate of 7.5 g/10 min (230°C, 2.16 kg) (Braskem, Brazil) was used as a polymer matrix. Hemp fibers were provided by AgroChanvre (France). Two hemp fibers loading, 10 wt% (PP10) and 30 wt% (PP30), were tested. Maleic anhydride grafted polypropylene (MA-g-PP), under the trademark Orevac CA100 (Arkema, France), was added at 3.1 wt% of PP as a coupling agent.

Process Conditions

Hemp fibers and MA-g-PP were dried for 15 h at 60°C. Then, granules of PP and MA-g-PP were mixed with hemp fibers in a BC21 Clextral twin-screw extruder (L/D = 36 with D = 25 mm) (Clextral, France) with the temperature profile 190-190-190-180-175-175-175°C and a screw speed of 220 rpm. Once dried for 3 days at 60°C, extruded pellets were injection molded into specimens in a Krauss Maffei machine (Krauss Maffei, Germany) at 210°C with an injection speed of 30 cm³·s⁻¹. Square samples of 100 mm × 100 mm × 2 mm were obtained.

Weathering Conditions

Samples were exposed from September 2015 to September 2016 in the south west of France under windshield glass to simulate a car interior environment according to ISO 877-2:2011 (Figure 1). The exposition panels were oriented toward the south at 45° with the ground. The interior environment was naturally ventilated thanks to holes located on stainless steel boxes 2 h per day. Temperature T(°C) and relative humidity RH(%) were

monitored and PP, PP10, and PP30 materials were sampled after 1, 2, 3, 6, 9, and 12 months. Temperatures ranged from -5°C in February to 91°C in August and relative humidity fluctuated between 3% in September and 95% in November.

Sampling and Analytical Methodology

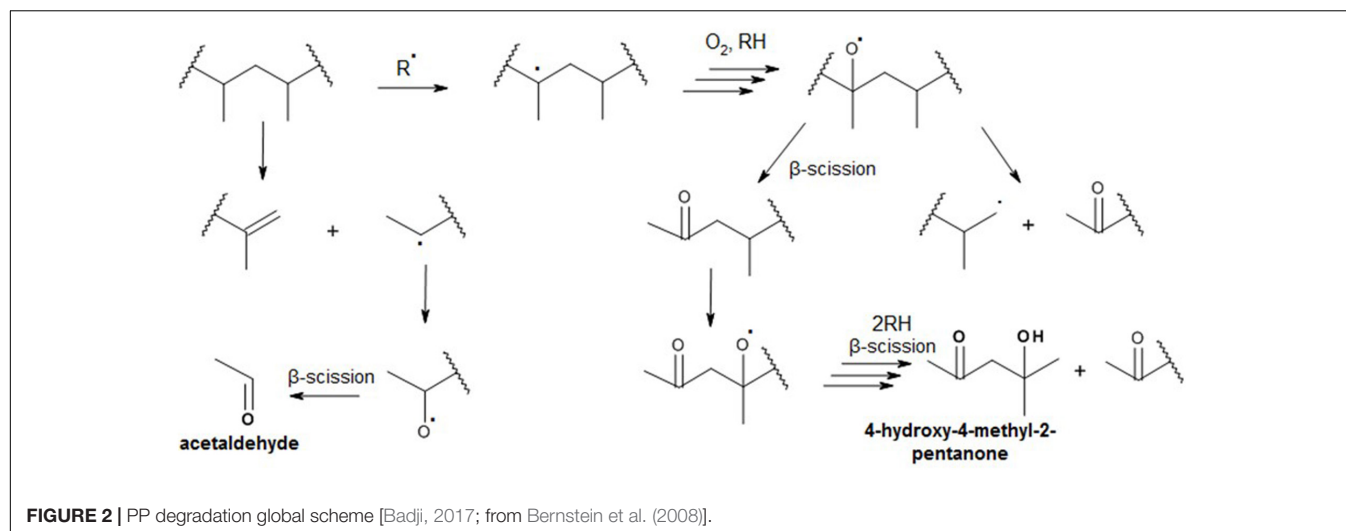
At each weathering step, three samples of each material were brought from the racks to the laboratory where VOCs emission analysis was carried out through a passive sampling method developed at the laboratory (Bourdin et al., 2014; Badji et al., 2018). It consists of two steps: firstly, a glass cell is placed on the material in order to isolate a part of its surface, and the VOCs are left to diffuse from the material to the air enclosed in the cell. When the VOCs concentration stabilizes, i.e., when material/air equilibrium is reached (Bourdin et al., 2014), a solid phase microextraction (SPME) fiber is introduced in the glass cell through a septum to sample emitted VOCs. Then, the SPME fiber is desorbed in the injector of a gas chromatograph (GC) coupled with mass spectrometer (MS) and flame ionization detector (FID; Varian, France) for identification and quantification of VOCs. The analytical procedure is detailed elsewhere (Bourdin and Desauziers, 2014). Both VOCs screening and specific analysis of formaldehyde and acetaldehyde, which are classified as carcinogen mutagenic and reprotoxic (CMR) substances, were performed (Chemical Risk Prevention Unit [CNRS], 2015). A polydimethylsiloxane–divinylbenzene–Carboxen fiber (PDMS/DVB/CAR, 50/30 μm) was selected for VOCs screening whereas a polydimethylsiloxane–divinylbenzene (PDMS/DVB, 65 μm) fiber impregnated with *O*-(2,3,4,5,6-pentafluorobenzyl)hydroxylamine hydrochloride (PFBHA) (Fluka, Switzerland) was used for formaldehyde and acetaldehyde (Kozziel et al., 2001; Bourdin and Desauziers, 2014). The SPME fibers were purchased from Supelco (United States). A sampling temperature of 80°C was tested to simulate extreme car interior conditions. The extraction time was fixed at 5 min.

Quantitative Analysis

The methodology described above allows for determining the concentration (in μg·m⁻³) of VOCs at the material/air interface. That concentration is related to the emission rate of the considered substance by the first Fick law of diffusion under steady state conditions (Wittkowski et al., 1992). For the screening analysis using a PDMS–DVB–CAR fiber, VOCs were quantified as toluene equivalent using an FID response since it is proportional to the effective carbon atoms number in the molecule (Fedoruk and Kerger, 2003). Furfural and 2-furanmethanol, compounds specific to hemp fibers and listed as CMR substances (Chemical Risk Prevention Unit [CNRS], 2015), as well as formaldehyde and acetaldehyde, were specifically quantified as described in a previous paper (Badji et al., 2018). Standard gases of formaldehyde and acetaldehyde were generated by a permeation device (Badji et al., 2018). For the other standard VOCs (toluene, furfural, and 2-furanmethanol), a continuous syringe injection method was used, as described elsewhere (Nicolle et al., 2008; Desauziers, 2004). The detection limit and quantification limit are around 8 and 23 μg·m⁻³, respectively for



FIGURE 1 | Under windshield glass exposure racks.



all compounds and the repeatability (relative standard deviation) is about 3% for three replicates.

RESULTS AND DISCUSSION

Polypropylene Oxidation

Some emitted VOCs were issued from the polymer degradation: long-chain aliphatic hydrocarbons and oxygenated products (linear ketones, aldehydes, and carboxylic acids). Acetic acid, acetone, and 2,4-pentanedione were the main compounds emitted by weathered PP. Some pathways are proposed in the literature to explain the formation of molecules containing a carbonyl functional group. Their mechanistic formation is found in literature (François-Heude et al., 2013; François-Heude et al., 2015). Mainly radical reactions lead to intermediate tertiary alkoxy radicals and their β -scission induces the previously identified carbonyl products (Figure 2). 2,4-pentanedione can result from the oxidation of methylketone issued from polymer chain reaction with unstable hydroperoxide. Moreover, 4-hydroxy-4-methyl-2-pentanone was also detected as high-level ketone (65 ± 13 and $82 \pm 25 \mu\text{g}\cdot\text{m}^{-3}$ for non-weathered and for one-year weathered PP, respectively (Badji et al., 2018)). It has been proposed that it originates from the same methyl ketone precursor. Indeed, the hydroxyl formation resulting from the alkoxy radical reaction with hydrogen followed by scission could form 4-hydroxy-4-methyl-2-pentanone.

Formaldehyde and acetaldehyde were also released by the polymer and biocomposites. Their levels increased with the time of exposure. A polymer degradation way, similar to previous oxygenated chemicals pathway, could explain acetaldehyde generation with secondary alkoxy radical initiator responsible for this low molecular compound formation. Moreover, formaldehyde generation is reported according to the mechanism of Hoff and Jacobsson, which consists of the oxidation of primary alkyl radicals (Hoff and Jacobsson, 1982).

Alcohols, resulting from polymer degradation, could arise from intermediate alkoxy radicals. However, abstracts

of a hydrogen from another molecule yields an hydroxyl group in tertiary carbon rather than a carbonyl group (Bernstein et al., 2008).

Cellulose and Hemicelluloses Degradation

Primary Decomposition

Two specifically quantified furan derivatives, furfural and 2-furanmethanol, were emitted at 1611 ± 20 and $2319 \pm 176 \mu\text{g}\cdot\text{m}^{-3}$, respectively by non-weathered PP30. Also, 5-methylfurfural ($660 \pm 30 \mu\text{g}\cdot\text{m}^{-3}$), 5-methyl-2(3H)-furanone ($40 \pm 14 \mu\text{g}\cdot\text{m}^{-3}$), furfuryl formate ($38 \pm 4 \mu\text{g}\cdot\text{m}^{-3}$), and furfuryl acetate ($43 \pm 4 \mu\text{g}\cdot\text{m}^{-3}$) evolved from biocomposites at the initial state. Apart from the last two compounds, these low molecular weight products were evidenced to be generated by holocellulose sequential degradation (Shen and Gu, 2009; Binder et al., 2010; Mäki-Arvela et al., 2012; Al-Shaal et al., 2015). Figure 3 shows the formation pathways of degradation products identified in this study and issued from the carbohydrate part of hemp fibers. The nominated products were those identified as VOCs issued from biocomposites. The carbohydrates' degradation under high temperature involves the depolymerization of polysaccharides by the glycosidic bonds cleavage between D-glucose units (Wang et al., 2012). This process is followed by dehydrations, leading to D-glucopyranose and D-xylofuranose formation. The formation of 2- or 5-substituted furans is generally explained to occur via glucopyranose ring-opening pathway with acyclic forms such as hexoses and pentoses intermediates (Sanders et al., 2003; Binder et al., 2010). The further cyclization of these oses leads to the furans formation. Primary subsequent dehydration steps produced specifically followed furfural and 2-furanmethanol emitted at high concentrations by non-weathered biocomposites. In this mechanistic scheme, other cyclic molecules were derived from hydroxymethylfurfural, which was not detected in the conditions of this study. Otherwise, the generation of

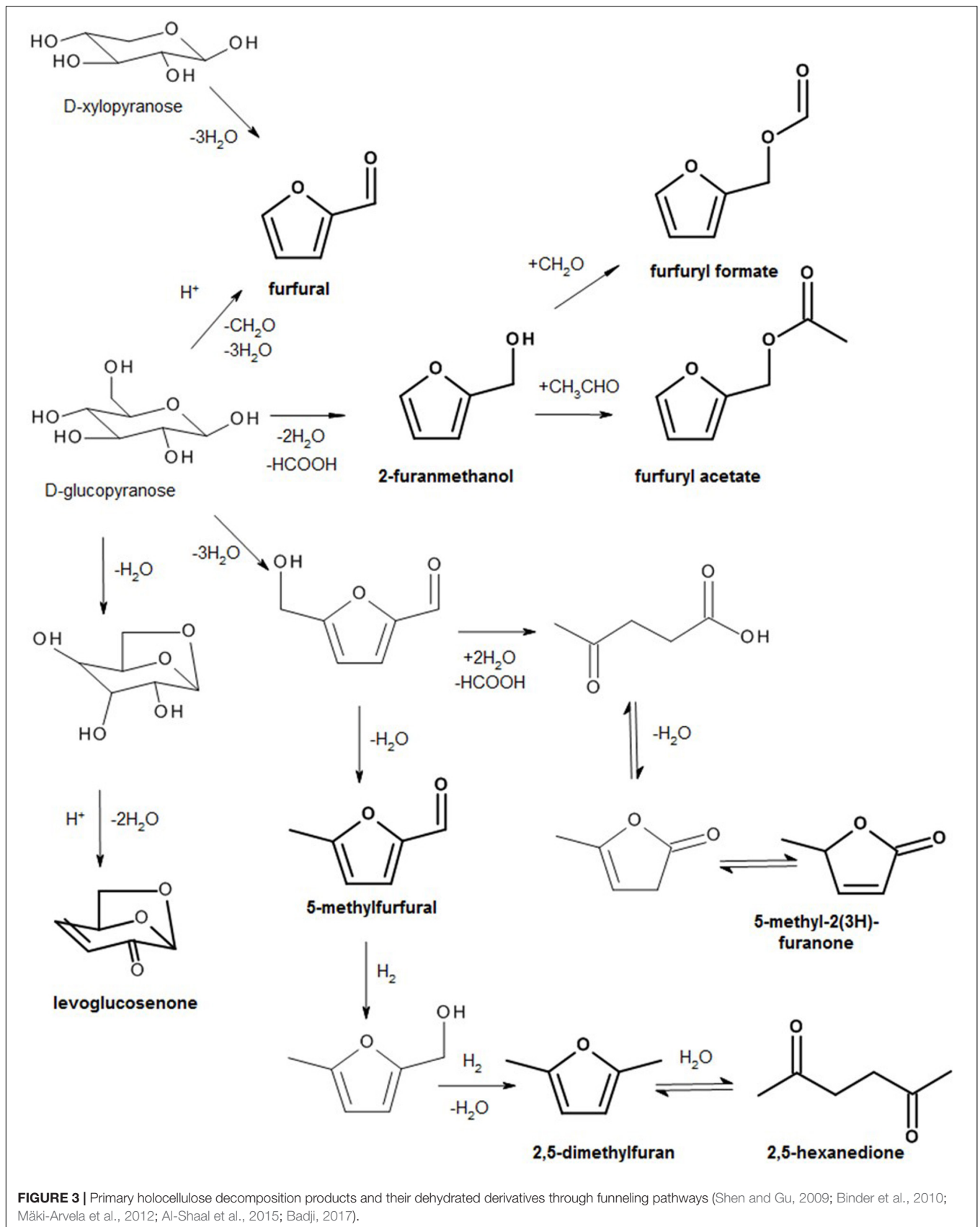
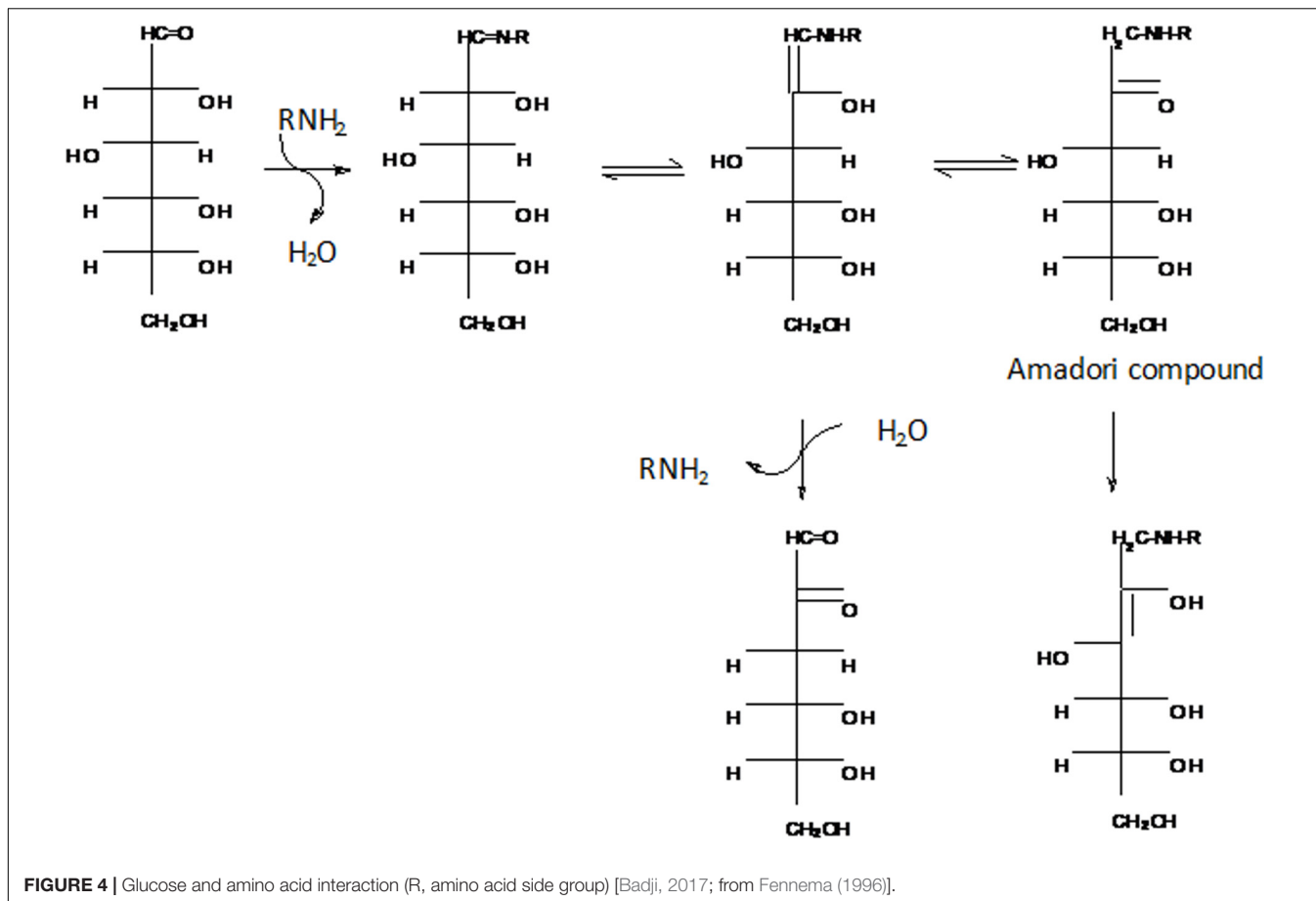


FIGURE 3 | Primary holocellulose decomposition products and their dehydrated derivatives through funneling pathways (Shen and Gu, 2009; Binder et al., 2010; Mäki-Arvela et al., 2012; Al-Shaal et al., 2015; Badji, 2017).



levoglucosenone ($97 \pm 4 \mu\text{g}\cdot\text{m}^{-3}$) derivative does not need the sugar ring-opening.

The products issued from the carbohydrate primary decomposition were mainly emitted by biocomposites at a non-weathered state. It has been supposed that generation could also be favored by Maillard reactions for which non-elevated temperatures (almost 100°C) are required (Newton et al., 2012) (chosen sampling temperature and those found in exposure racks do not exceed 91°C), contrary to the pyrolysis method. Indeed, until now, Maillard reactions have not supported the degradation pathways of vegetal fibers. However, either 1,2- or 2,3-enolization of the Amadori compound, previously mentioned in the introductory part, rising from aldoses such as glucose could effectively lead to furfural and hydroxymethylfurfural. Indeed, these compounds were already explained to originate from sugar-containing food, such as lactose, through Maillard reactions (Newton et al., 2012). But the same mechanism could justify the formation of the products detected here. Also, further intermediate dicarbonyls (reductones) formed after intrarearrangement (enolization) are responsible for the autocatalytic character of the Maillard reaction (Figure 4). Moreover, as mentioned in the introductory part, proteins present in fibers could allow the glycosylamine precursor formation required for obtaining advanced Maillard reaction products. Otherwise, their presence is demonstrated by the detection of pyrazines

emitted by biocomposites (methylpyrazine and N-acetyl-4(H)-pyridine at 25 ± 2 and $38 \pm 4 \mu\text{g}\cdot\text{m}^{-3}$, respectively for PP30). These secondary products of Strecker degradation are due to aminoketones condensation.

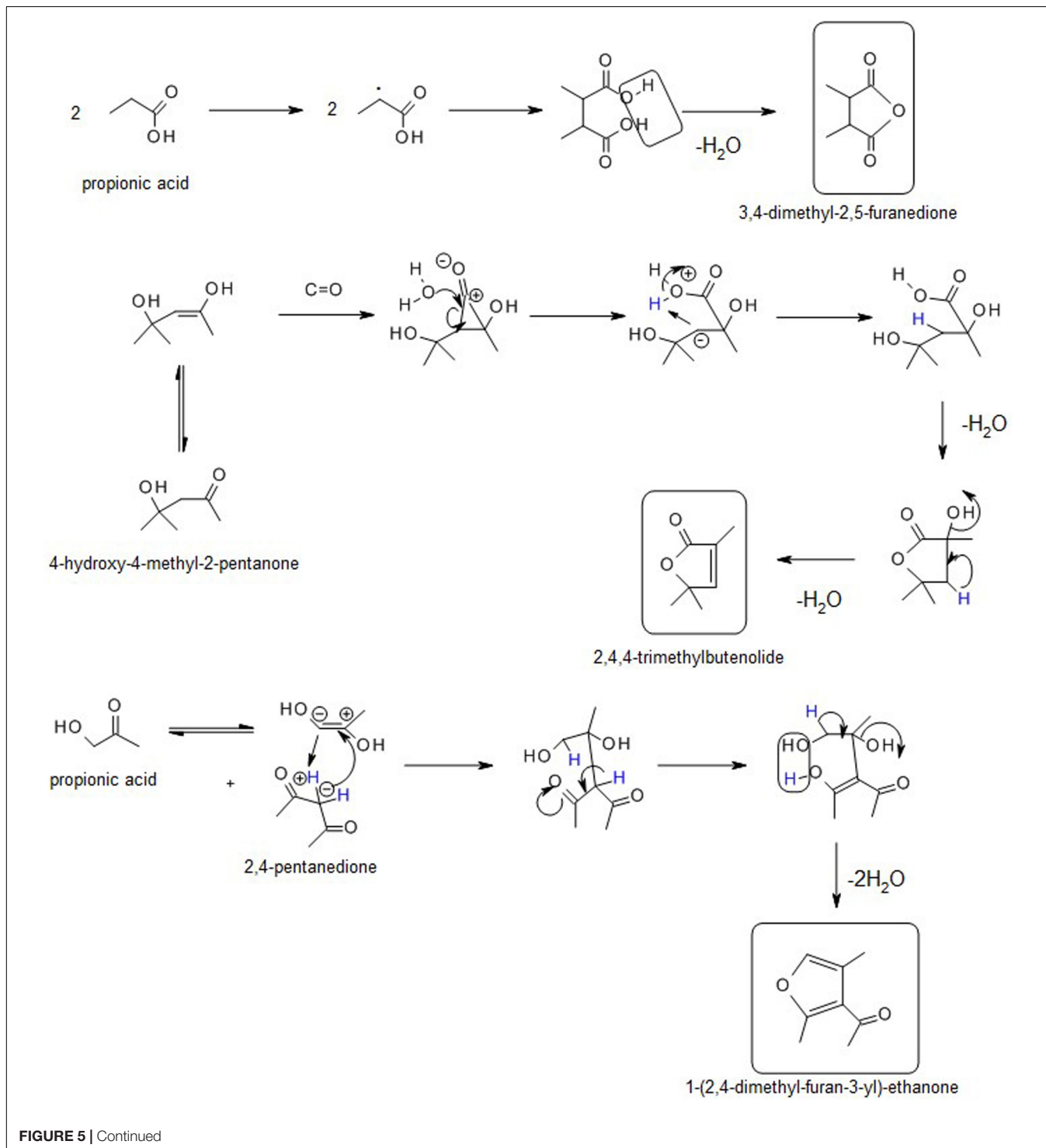
Contrary to other compounds, the formation of furfuryl formate and furfuryl acetate (total concentration of $81 \pm 8 \mu\text{g}\cdot\text{m}^{-3}$) aroused from non-weathered PP30 composite has not been reported in the literature. Here, it is suggested that they result from the interaction between the hydroxy functional groups of 2-furanmethanol and formaldehyde and acetaldehyde, respectively (Figure 3). Formaldehyde and acetaldehyde could also evolve from the Strecker degradation (Hodge et al., 1972; Newton et al., 2012) by β -scission. Indeed, for biocomposites, lots of aliphatic ketones and aldehydes such as 1-hydroxy-2-propanone, 1-acetyloxy-2-propanone, and nonanal are emitted at the highest levels of their chemical family: 420 ± 81 , 366 ± 11 , and $160 \pm 28 \mu\text{g}\cdot\text{m}^{-3}$, respectively, for unaged PP30. They were identified as hemp fibers by-products at a non-weathered state. These by-products could be linked to the reaction between amino acids and two-carbonyl compounds.

Secondary Decomposition

After weathering, mainly methyl substituted furanones deriving from carbohydrates were formed. They represented 13% of the level of ketones released by PP30 after one year of weathering,

whereas they only accounted for 8% of ketones by-products emitted by non-weathered PP30. Moreover, contrary to a non-weathered state, only furans compounds containing at least one substitution in 3 and 4 positions were identified after weathering. In addition, contrary to 2- and 5-substituted furanones presented in **Figure 3**, the explanation of 3- or 4-substituted furanones

issued from vegetal fibers decomposition has not yet been reported in the literature. The proposed reactions featured in **Figure 5** involve the interaction between functional groups of identified volatile products. Substances that are designed by their names in **Figure 5** correspond to substances detected in this work. The first reaction (1) implies a radical attack in α position of



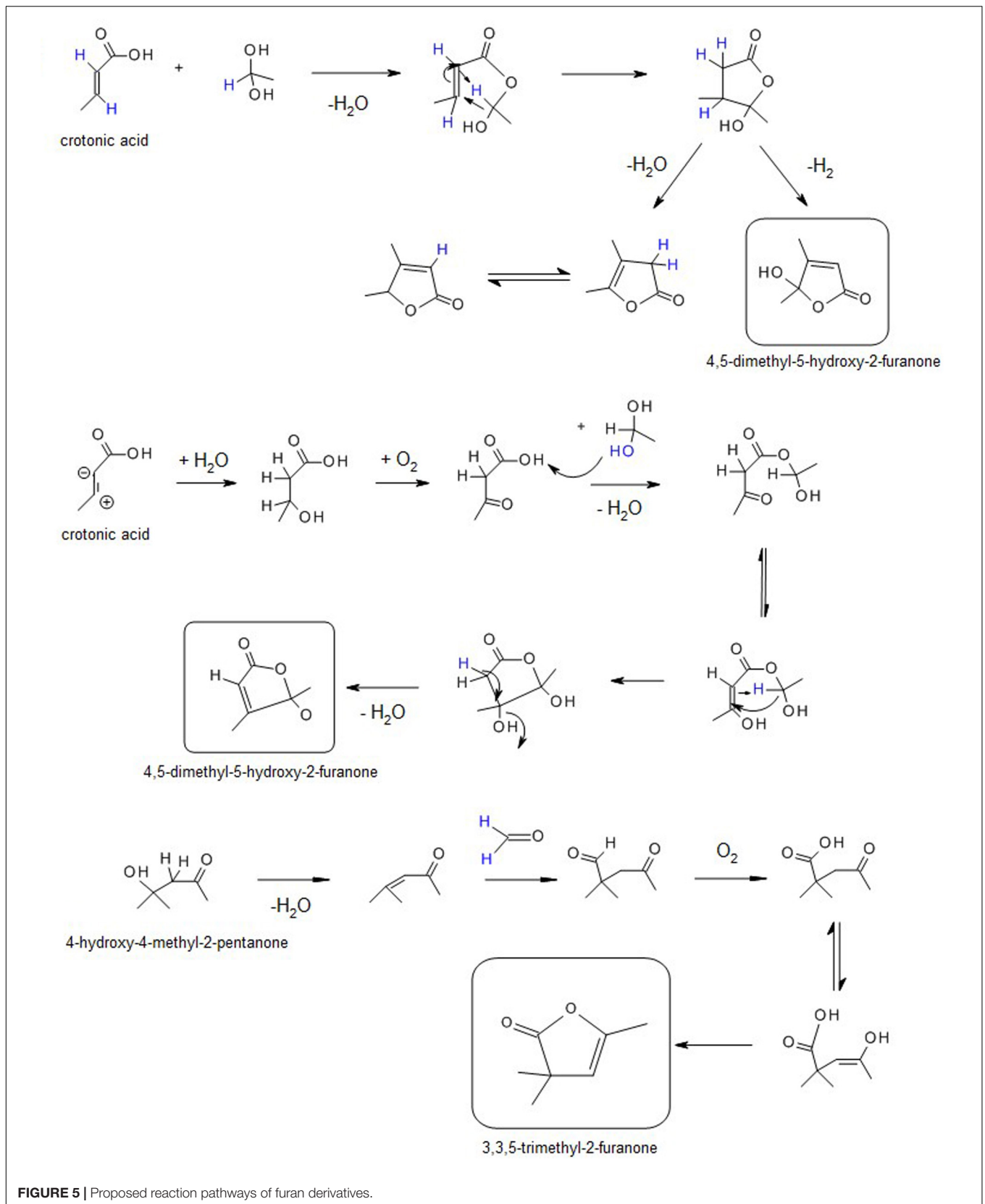


FIGURE 5 | Proposed reaction pathways of furan derivatives.

two identical propionic acid by-products, whose levels increased from 39 ± 4 to $839 \pm 75 \mu\text{g}\cdot\text{m}^{-3}$ and 56 ± 16 to $1403 \pm 3 \mu\text{g}\cdot\text{m}^{-3}$ for PP10 and PP30, respectively, via a photo-chemical method caused by ultraviolet (UV) rays. It is followed by the dehydration of the generated intermediate symmetrical molecule leading to an intramolecular cyclization giving 3,4-dimethyl-2,5-furanedione ($118 \pm 32 \mu\text{g}\cdot\text{m}^{-3}$ for weathered PP30).

The reaction (2) occurs through the establishment of a keto-enolization equilibrium thermodynamically driven between the keto and enol forms of 4-hydroxy-4-methyl-2-pentanone (**Figure 5**). Moreover, this ketone was detected at an extremely high concentration after weathering (until almost $3000 \mu\text{g}\cdot\text{m}^{-3}$ for PP30 after 12 months), especially for biocomposites. Then, the attack of the enone form via C=C hydroformylation by carbon monoxide leads to an instable compound formation. Its further hydrolysis induces a cyclopropane ring-opening. Thus, these two previous steps lead to the functionalization of a formic acid group. Then, two successive dehydrations firstly induce a cyclization into 2-furanone structure. After, the dehydroxylation in the 3-position induces a double bond formation to generate 2,4,4-trimethylbut-2-enolide. This volatile compound was emitted at the highest concentration of the 2-furanones group after one year of weathering. Indeed, since the group of 2-furanones products was emitted at $3285 \pm 666 \mu\text{g}\cdot\text{m}^{-3}$ by PP30 weathered for one year, 2,4,4-trimethylbut-2-enolide accounted for almost 40% ($1314 \pm 30 \mu\text{g}\cdot\text{m}^{-3}$) for PP30 weathered for one year. This can be explained by the extremely high concentration of the 4-hydroxy-4-methyl-2-pentanone reactant previously mentioned, giving way to the formation of 2,4,4-trimethylbut-2-enolide.

1-(2,4-dimethyl-furan-3-yl)-ethanone, whose generation ($1063 \pm 243 \mu\text{g}\cdot\text{m}^{-3}$ for PP30 and $1807 \pm 149 \mu\text{g}\cdot\text{m}^{-3}$ for PP10) is explained in pathway (3) of **Figure 5**, implies the reaction between propionic acid and 2,4-pentanedione, two volatile compounds emitted in high quantities. Indeed, propionic acid was emitted at almost 800 and $1400 \mu\text{g}\cdot\text{m}^{-3}$ for PP10 and PP30, respectively, and a concentration of almost $7300 \mu\text{g}\cdot\text{m}^{-3}$ of the 2,4-pentanedione was recorded for the two biocomposites after one year. The highly reactive C = C formed through keto-enolization tautomerism of propionic acid is opened by C3 of the diketone. Then, a further keto-enolization of the intermediate compound hydroxydiketone derivative is established and precedes dehydrations occurring in the final stage.

As regards reaction (4.1) shown in **Figure 5**, the esterification of crotonic acid favored by the condensation of ethanol hydrate hydroxyl group, a molecule easily generated from acetaldehyde hydration on crotonic acid, is followed by the removal of a water molecule. The C-C double bond initially present is opened after cyclization. This produces a 4-hydroxy-4,5-dimethyl-2-furanone. However, as it is difficult for the possible further dehydrogenation process to occur, the reaction (4.2) is an alternative to (4.1) that requires more energy than (4.2). This generates the previously explained structure (4-hydroxy-4,5-dimethyl-2-furanone) at the final stage. A similar esterification way of the diketone intermediate product, followed by a cyclization and dehydration, could explain its formation.

The same precursors as found in reaction (2) may be responsible for the 5-hydroxy-3,3,5-trimethyl-2-furanone formation [pathway (5) of **Figure 5**]. Indeed, the dehydration and hydroformylation of the methylpentanone due to its reactions with CO and O₂ lead to methyl substituted levulinic acid generation, a well-known biomass derivative (Al-Shaal et al., 2015), that finally cyclizes after its keto-enolization.

Some of these reactions may require high energy conditions to occur. However, the biomass inorganic part contains metals which could catalyze these reactions (Nowakowski and Jones, 2008).

Lignin Degradation

Primary Decomposition

Two methoxy-substituted phenols, vanillin and 4-vinylguaiacol, were emitted by non-weathered biocomposites. These two compounds are thought to originate from a primary decomposition of lignin favored in the heating conditions of ferulic acid, a well-known by-product evolving from lignin degradation, but not identified in this study (Coghe et al., 2004; Peleg et al., 1992).

Firstly, decarboxylation of ferulic acid may cause the formation of vinylguaiacol through (1.1) pathway (**Figure 6**; Coghe et al., 2004). Indeed, it is reported that temperatures ranging from 100 to 250°C (including the process temperature) cause severe damage to natural fibers' chemical structure through depolymerization, dehydration, or decarboxylation (Gassan and Bledzki, 2001). Vanillin is known to originate from the oxidation of 4-vinylguaiacol issued from lignin (1.2). The literature also proposed vanillin arises through the hydrolysis of the ferulic acid by-product (2.1) (Peleg et al., 1992). A further deacetylation could induce the formation of vanillin (2.2). This pathway could occur more easily than the vinylguaiacol or eugenol oxidation. Indeed, even if the decarboxylation consists in a naturally occurring step, the oxidation of carbon-carbon double bond must be catalyzed. Moreover, it has been shown that (2) pathways preferentially

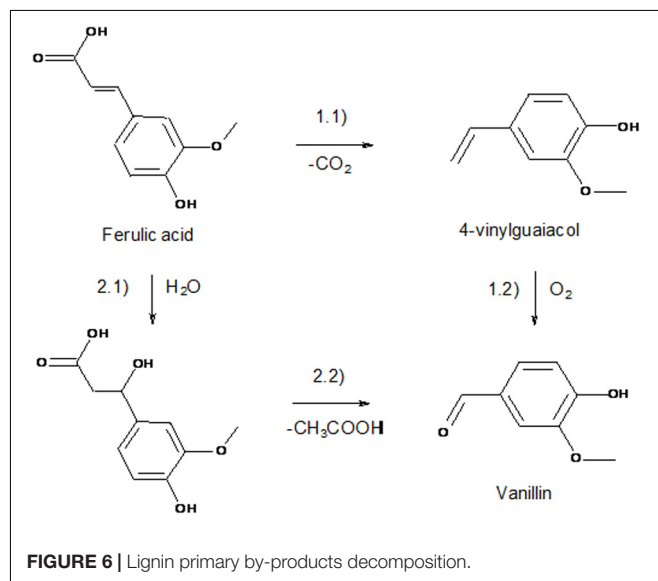


FIGURE 6 | Lignin primary by-products decomposition.

occur for obtaining vanillin than (1) ones (Peleg et al., 1992). Otherwise, the presence of metalloproteins containing iron, copper, and manganese might catalyze the by-products formation (Pollegioni et al., 2015).

Secondary Decomposition

3,5-dimethylphenol (3,5-xylénol) was continuously emitted by biocomposites during the weathering. It rose from $94 \pm 30 \mu\text{g}\cdot\text{m}^{-3}$ after 1 month to $471 \pm 75 \mu\text{g}\cdot\text{m}^{-3}$ (PP30) after 12 months of exposition for PP30. At high temperatures, these alkylated phenols are formed by C–O radical cleavage of the methoxy group and further coupling of phenolic radical with the methyl radical group (Wittkowski et al., 1992). However, alkylphenols can appear easily only under pyrolysis conditions of lignin allowing alkylation. In our study, the temperature conditions are not favorable enough to trigger methylation. Nevertheless, as discussed previously, several factors could still contribute to alkylphenols sourcing. Indeed, brown and white-root fungi are recognized to be able to demethoxylate lignin (Lopretti et al., 1998). Moreover, UV radiation leading to demethoxylation (Hon and Chang, 1984; Srinivas and Pandey, 2012) may explain the formation of xylénol emitted only once biocomposites were exposed to climatic conditions. In this work, it has been assumed that this abstraction can give way to combinations between methyl radicals issued from the demethylation of lignin allowed by O-demethylase enzymes active before the hemp fibers process (Peng et al., 2002) and phenol radical. Moreover, enzymes present in lignin and included in proteins could play the role of natural biocatalysts of these reactions before the process of biocomposites (Pollegioni et al., 2015). In addition, the retting process could favor micro-organisms formation, thereby accelerating by-products generation.

CONCLUSION

Since biocomposites are becoming more and more integrated in vehicles, knowledge about their aging and related mechanisms is needed. Therefore, the aim of this work was to rely on the structure of VOCs issued from non-weathered and under-glass-weathered PP and hemp fibers reinforced biocomposites to understand their degradation pathways. Reaction schemes were proposed according to volatile products that were identified in this study accordingly to an original and non-destructive sampling method.

REFERENCES

- Ahmad, T., Maa, Z., Mohd Ishak, Z. A., Mat Taib, R., Rahim, S., and Jani, S. M. (2011). Natural Weathering of Kenaf Bast Fibre-Filled Poly(Butylene Succinate) Composites: effect of Fibre Loading and Compatibiliser Addition. *J. Polym. Environ.* 19, 263–273. doi: 10.1007/s10924-010-0272-2
- Air quality sciences Inc. (2006). *Indoor Air Quality Hazards of New Cars*. Marietta, GA: Air quality sciences Inc, 47–51.
- Al-Shaal, M. G., Ciptonugroho, W., Holzhäuser, F. J., Mensah, J. B., Hausoul, P. J. C., and Palkovits, R. (2015). Catalytic Upgrading of α -Angelica Lactone to Levulinic Acid Esters under Mild Conditions over Heterogeneous Catalysts. *Catal. Sci. Technol.* 5, 5168–5173. doi: 10.1039/C5CY00446B
- Azwa, Z. N., Yousif, B. F., Manalo, A. C., and Karunasena, W. (2013). A Review on the Degradability of Polymeric Composites Based on Natural Fibres. *Mater. Design* 47, 424–442. doi: 10.1016/j.matdes.2012.11.025
- Badji, C. (2017). *Viellissement de Matériaux Composites Renforcés de Fibres Naturelles: Étude de l'impact Sur Les Propriétés d'aspect et Sur Les Émissions Dans l'air Intérieur*. France: Université de Pau et des Pays de l'Adour.
- Badji, C., Beigbeder, J., Garay, H., Bergeret, A., Bénézet, J. C., and Desauziers, V. (2018). Under Glass Weathering of Hemp Fibers reinforced polypropylene biocomposites: impact of volatile organic compounds emissions on indoor air

Firstly, it was assumed that the primary decomposition of holocellulose and lignin in hemp fibers occurred at a non-weathered state whereas secondary decomposition was favored at a weathered state. Mainly 2- and 5-substituted furans were emitted by non-weathered biocomposites. Since the same precursors and the same nitrogen-containing chemicals evolved from non-weathered vegetal fibers decomposition as food thermal degradation, Maillard mechanism could be extrapolated to this study. 3-, 4-, and 5-substituted furanones were preferentially emitted after weathering. Some reactions between volatile products were proposed: they mainly involved keto-enolization, dehydration, and cyclization mechanisms. As regards lignin decomposition, methoxyphenols, detected at a non-weathered state, were explained by hydration and oxidation whereas dimethylphenol, evolved from weathered biocomposites, could originate from radical reactions.

However, the reactions implying dehydrogenation that produce 4,5-dimethyl-5-hydroxy-2-furanone (cellulose) and oxidation of vinyl specie to give vanillin (lignin) need highly favorable conditions to occur. Thus, activation energy calculation of the proposed reactions could be further modeled to check their occurrence feasibility. Also, the precise role of proteins and enzymes in carbohydrates and lignin degradation must be more deeply investigated. Additives such as light stabilizers or antioxidants incorporated in the materials can be used to limit dehydrations inducing sugar ring-opening and the impact of exposition to UV rays and high temperatures.

DATA AVAILABILITY STATEMENT

The datasets generated for this study are available on request to the corresponding author.

AUTHOR CONTRIBUTIONS

CB was the head of the whole project and drafted the manuscript. J-MS gave his expertise on the chemical pathways determination. HG helped for the weathering experiments. JB helped for VOCs measurements. AB and J-CB supervised the hemp fiber composite design and fabrication. VD was expert for the whole projet, designing it and supervising the COVs measurements. All the authors read and approved the manuscript.

- quality. *Polym. Degrad. Stabil.* 149, 85–95. doi: 10.1016/j.polymdegradstab.2018.01.020
- Badji, C., Soccalingame, L., Garay, H., Bergeret, A., and Bénézet, J.-C. (2017). Influence of weathering on visual and surface aspect of wood plastic composites: correlation approach with mechanical properties and microstructure. *Polym. Degrad. Stabil.* 137, 162–172. doi: 10.1016/j.polymdegradstab.2017.01.010
- Belitz, H.-D., Grosch, W., and Schieberle, P. (2004). "Aroma compounds," in *Food Chemistry*, ed. M. Dekker (Boca Raton, FL: CRC Press), 340–402. doi: 10.1007/978-3-662-07279-0
- Bernstein, R., Thornberg, S. M., Irwin, A. N., Hochrein, J. M., Derzon, D. K., Klamo, S. B., et al. (2008). Radiation-oxidation mechanisms: volatile organic degradation products from polypropylene having selective C-13 labeling studied by GC/MS. *Polym. Degrad. Stabil.* 93, 854–870. doi: 10.1016/j.polymdegradstab.2008.01.020
- Binder, J. B., Blank, J. J., Cefali, A. V., and Raines, R. T. (2010). Synthesis of Furfural from Xylose and Xylan. *ChemSusChem* 3, 1268–1272. doi: 10.1002/cssc.201000181
- Bourdin, D., and Desauziers, V. (2014). Development of SPME On-Fiber Derivatization for the Sampling of Formaldehyde and Other Carbonyl Compounds in Indoor Air. *Anal. Bioanal. Chem.* 406, 317–328. doi: 10.1007/s00216-013-7460-6
- Bourdin, D., Mocho, P., Desauziers, V., and Plaisance, H. (2014). Formaldehyde emission behavior of building materials: on-site measurements and modeling approach to predict indoor air pollution. *J. Hazard. Mater.* 280, 164–173. doi: 10.1016/j.jhazmat.2014.07.065
- Brzonova, I., Kozliak, E., Kubátová, A., Chebeir, M., Qin, W., Christopher, L., et al. (2014). "Kenaf Biomass Biodecomposition by Basidiomycetes and Actinobacteria in Submerged Fermentation for Production of Carbohydrates and Phenolic Compounds. *Bioresour. Technol.* 173, 352–360. doi: 10.1016/j.biortech.2014.09.057
- Carrier, M., Loppinet-Serani, A., Absalon, C., Aymonier, C., and Mench, M. (2012). Degradation Pathways of Holocellulose, Lignin and Alpha-Cellulose from *Pteris Vittata* fronds in sub- and super critical conditions. *Biomass Bioenergy* 43, 65–71. doi: 10.1016/j.biombioe.2012.03.035
- Chemical Risk Prevention Unit [CNRS] (2015). *European Harmonised Classification and Labelling of Carcinogenic, Mutagenic and Toxic for Reproduction (CMR) Substances According to the Criteria of the CLP Regulation*. Paris: CNRS.
- Coghe, S., Benoot, K., Delvaux, F., Vanderhaegen, B., and Delvaux, F. R. (2004). "Ferulic Acid Release and 4-Vinylguaiaicol formation during brewing and fermentation: indications for Feruloyl esterase activity in *Saccharomyces cerevisiae*. *J. Agric. Food Chem.* 52, 602–608. doi: 10.1021/jf0346556
- Desauziers, V. (2004). Traceability of Pollutant Measurements for Ambient Air Monitoring. *Trends Anal. Chem.* 23, 252–260. doi: 10.1016/S0165-9936(04)00310-3
- Dorez, G., Taguet, A., Ferry, L., and Lopez-Cuesta, J. M. (2013). Thermal and fire behavior of natural Fibers/PBS biocomposites. *Polym. Degrad. Stabil.* 98, 87–95. doi: 10.1016/j.polymdegradstab.2012.10.026
- Fedoruk, M. J., and Kerger, B. D. (2003). Measurement of volatile organic compounds inside automobiles. *J. Expo. Anal. Environ. Epidemiol.* 13, 31–41. doi: 10.1038/sj.jea.7500250
- Fennema, O. R. (1996). *Food Chemistry*, 3rd Edn, ed. M. Dekker (Boca Raton, FL: CRC Press).
- François-Heude, A., Richaud, E., Desnoux, E., and Colin, X. (2014). Influence of Temperature, UV-Light wavelength and intensity on polypropylene photothermal oxidation. *Polym. Degrad. Stabil.* 100, 10–20. doi: 10.1016/j.polymdegradstab.2013.12.038
- François-Heude, A., Richaud, E., Desnoux, E., and Colin, X. (2015). A general kinetic model for the Photothermal Oxidation of polypropylene. *J. Photochem. Photobiol. A* 296, 48–65. doi: 10.1016/j.jphotochem.2014.08.015
- François-Heude, A., Richaud, E., Leprovost, J., Heninger, M., Mestdagh, H., Desnoux, E., et al. (2013). Real-Time quantitative analysis of volatile products generated during solid-state Polypropylene thermal oxidation. *Polym. Testing* 32, 907–917. doi: 10.1016/j.polymertesting.2013.04.008
- Gassan, J., and Bledzki, A. K. (2001). Thermal Degradation of Flax and Jute Fibers. *J. Appl. Polym. Sci.* 82, 1417–1422. doi: 10.1002/app.1979
- He, C., Chen, C. L., Giannis, A., Yang, Y., and Wang, J. Y. (2014). Hydrothermal Gasification of Sewage Sludge and Model Compounds for Renewable Hydrogen Production: a Review. *Renew. Sustain. Energy Rev.* 39, 1127–1142. doi: 10.1016/j.rser.2014.07.141
- Hodge, J. E., Mills, F. D., and Fisher, B. E. (1972). Compounds of browned flavor derived from sugar-amine reactions. *Am. Assoc. Cereal Chem.* 17, 34–40.
- Hoff, A., and Jacobsson, S. (1982). Thermal oxidation of Polypropylene close to industrial processing conditions. *J. Appl. Polym. Sci.* 27, 2539–2551. doi: 10.1002/app.1982.070270723
- Hon, D. N.-S., and Chang, S.-T. (1984). Surface degradation of wood by ultraviolet light. *J. Polym. Sci.* 22, 2227–2241. doi: 10.1002/pol.1984.170220923
- John, M., and Thomas, S. (2008). Biofibres and biocomposites. *Carbohydr. Polym.* 71, 343–364. doi: 10.1016/j.carbpol.2007.05.040
- Katō, K., and Komorita, H. (1968). Pyrolysis of cellulose. *Agricult. Biol. Chem.* 32, 21–26. doi: 10.1080/00021369.1968.10859016
- Khazaeian, A., Ashori, A., and Dizaj, M. Y. (2015). Suitability of Sorghum stalk fibers for production of particleboard. *Carbohydr. Polym.* 120, 15–21. doi: 10.1016/j.carbpol.2014.12.001
- Kim, H.-S., Kim, S., Kim, H.-J., and Kim, H.-G. (2006). Physico-Mechanical Properties, Odor and VOC Emission of Bio-Flour-Filled Poly(Propylene) Bio-Composites with Different Volcanic Pozzolan contents. *Macromol. Mater. Eng.* 291, 1255–1264. doi: 10.1002/mame.200600212
- Kim, H.-S., Lee, B.-H., Kim, H.-J., and Yang, H.-S. (2011). Mechanical-Thermal Properties and VOC emissions of natural-flour-filled biodegradable polymer hybrid bio-composites. *J. Polym. Environ.* 19:628. doi: 10.1007/s10924-011-0313-5
- Koziel, J. A., Noah, J., and Pawliszyn, J. (2001). Field sampling and determination of Formaldehyde in indoor air with solid-phase Microextraction and on-Fiber Derivatization. *Environ. Sci. Technol.* 35, 1481–1486. doi: 10.1021/es001653i
- Kumre, A., Rana, R. S., and Purohit, R. (2017). A review on mechanical property of sisal glass Fiber Reinforced polymer composites. *Mater. Today* 4, 3466–3476. doi: 10.1016/J.MATPR.2017.02.236
- Liu, Y., and Hu, H. (2008). X-Ray Diffraction Study of Bamboo Fibers Treated with NaOH. *Fibers Polym.* 9, 735–739. doi: 10.1007/s12221-008-0115-0
- Lopretti, M., Cabella, D., Morais, J., and Rodrigues, A. (1998). Demethoxylation of Lignin-Model Compounds with Enzyme Extracts from *Gloeophillum Trabeum*. *Process Biochem.* 33, 657–661. doi: 10.1016/S0032-9592(98)00028-4
- Mäki-Arvela, P., Salminen, E., Riittinen, T., Virtanen, P., Kumar, N., and Mikkola, J. P. (2012). The Challenge of Efficient Synthesis of Biofuels from Lignocellulose for future renewable transportation fuels. *Int. J. Chem. Eng.* 2012:674761. doi: 10.1155/2012/674761
- Mitsuo, N. (1988). "Chemistry of Maillard reactions: recent studies on the browning reaction mechanism and the development of antioxidants and mutagens," in *Advances in Food Research*, Vol. 32, eds C. O. Chichester and B. S. Schweigert (Amsterdam: Elsevier Inc), 116–143.
- Muasher, M., and Sain, M. (2006). The efficacy of photostabilizers on the color change of wood filled plastic composites. *Polymer Degrad. Stabil.* 91, 1156–1165. doi: 10.1016/j.polymdegradstab.2005.06.024
- Newton, A. E., Fairbanks, A. J., Golding, M., Andrewes, P., and Gerrard, J. A. (2012). The Role of the Maillard Reaction in the formation of flavour compounds in dairy products - not only a deleterious reaction but also a rich source of flavour compounds. *Food Funct.* 3, 1231–1241. doi: 10.1039/c2fo30089c
- Nicolle, J., Desauziers, V., and Mocho, P. (2008). Solid Phase Microextraction sampling for a rapid and simple on-site evaluation of volatile organic compounds emitted from building materials. *J. Chromatogr. A* 1208, 10–15. doi: 10.1016/j.chroma.2008.08.061
- Nowakowski, D. J., and Jones, J. M. (2008). Uncatalysed and Potassium-catalysed pyrolysis of the cell-wall constituents of biomass and their model compounds. *J. Anal. Appl. Pyroly.* 83, 12–25. doi: 10.1016/j.jaap.2008.05.007
- Peleg, H., Naim, M., Zehavi, U., Rouseff, R. L., and Nagy, S. (1992). Pathways of 4-Vinylguaiaicol Formation from Ferulic Acid in Model Solutions of Orange Juice. *J. Agric. Food Chem.* 40, 764–767. doi: 10.1021/jf00017a011
- Peng, X., Masai, E., Kitayama, H., Harada, K., Katayama, Y., and Fukuda, M. (2002). Characterization of the 5-Carboxyvanillate Decarboxylase Gene and Its Role in Lignin-Related Biphenyl Catabolism in *Sphingomonas Paucimobilis* SYK-6. *Appl. Environ. Microbiol.* 68, 4407–4415. doi: 10.1128/AEM.68.9.4407

- Peng, Y., and Wu, S. (2011). Fast pyrolysis characteristics of sugarcane bagasse hemicellulose. *Cell. Chem. Technol.* 45, 605–612.
- Perez, R. F., and Fraga, M. A. (2014). Hemicellulose-derived chemicals: one-step production of furfuryl alcohol from Xylose. *Green Chem.* 16:3942. doi: 10.1039/C4GC00398E
- Pollegioni, L., Tonin, F., and Rosini, E. (2015). Lignin-degrading enzymes. *FEBS J.* 282, 1190–1213. doi: 10.1111/febs.13224
- Rabek, J. F. (1990). *Photostabilization of Polymers: Principles and Applications*. Amsterdam: Elsevier, doi: 10.1007/978-94-009-07-47-8
- Rouillon, C., Bussiere, P. O., Desnoux, E., Collin, S., Vial, C., Therias, S., et al. (2016). Is Carbonyl Index a Quantitative Probe to Monitor Polypropylene Photodegradation? *Polym. Degrad. Stabil.* 128, 200–208. doi: 10.1016/j.polymdegradstab.2015.12.011
- Saba, N., Jawaid, M., Alothman, O. Y., and Paridah, M. T. (2016). A review on dynamic mechanical properties of natural fibre reinforced polymer composites. *Construct. Build. Mater.* 106, 149–159. doi: 10.1016/J.CONBUILDMAT.2015.12.075
- Sanders, E. B., Goldsmith, A. I., and Seeman, J. I. (2003). A Model That Distinguishes the Pyrolysis of D-Glucose, d-Fructose, and sucrose from that of cellulose. application to the understanding of cigarette smoke formation. *J. Anal. Appl. Pyrolys.* 66, 29–50. doi: 10.1016/S0165-2370(02)00104-3
- Sari, Y. W. (2015). *Biomass and Its Potential for Protein and Amino Acids; Valorizing Agricultural by-Products*. PhD thesis, Wageningen University, Wageningen.
- Shen, D. K., and Gu, S. (2009). The mechanism for thermal decomposition of cellulose and its main products. *Bioresour. Technol.* 100, 6496–6504. doi: 10.1016/j.biortech.2009.06.095
- Shibata, S. (2016). *Natural Fiber Composites*. Amsterdam: Elsevier, 157–173.
- Srinivas, K., and Pandey, K. K. (2012). Photodegradation of Thermally Modified Wood. *J. Photochem. Photobiol. B* 117, 140–145. doi: 10.1016/j.jphotobiol.2012.09.013
- Van Schoors, L., Gueguen, M. M., Moscardelli, S., Rabii, H., and Davies, P. (2018). Antioxidant Properties of Flax Fibers in Polyethylene matrix composites. *Indus. Crops Products* 126, 333–339. doi: 10.1016/J.INDCROP.2018.09.047
- Wang, S., Guo, X., Liang, X. T., Zhou, Y., and Luo, Z. (2012). Mechanism research on cellulose Pyrolysis by Py-GC/MS and subsequent density functional theory studies. *Bioresour. Technol.* 104, 722–728. doi: 10.1016/j.biortech.2011.10.078
- Wittkowski, R., Ruther, J., Drinda, H., and Rafiei-Taghanaki, F. (1992). Formation of Smoke Flavor Compounds by Thermal Lignin Degradation. *ACS Symposium Series* 490, 232–243. doi: 10.1021/bk-1992-0490.ch018
- Yu, C., and Crump, D. (1998). A review of the emission of VOCs from Polymeric materials used in buildings. *Build. Environ.* 33, 357–374. doi: 10.1016/S0360-1323(97)00055-3
- Zhang, Q., Ames, J. M., Smith, R. D., Baynes, J. W., and Metz, T. O. (2008). A perspective on the Maillard reaction and the analysis of protein Glycation by mass spectrometry: probing the pathogenesis of Chronic disease. *J. Proteome Res.* 8, 754–769. doi: 10.1021/pr800858h
- Zou, P., Xiong, H., and Tang, S. (2008). Natural Weathering of Rape Straw Flour (RSF)/HDPE and Nano-SiO₂/RSF/HDPE composites. *Carbohydr. Polymers* 73, 378–383. doi: 10.1016/j.carbpol.2007.12.002

Conflict of Interest: The authors declare that the research was conducted in the absence of any commercial or financial relationships that could be construed as a potential conflict of interest.

Copyright © 2020 Badji, Sotiropoulos, Beigbeder, Garay, Bergeret, Bénézet and Desauziers. This is an open-access article distributed under the terms of the Creative Commons Attribution License (CC BY). The use, distribution or reproduction in other forums is permitted, provided the original author(s) and the copyright owner(s) are credited and that the original publication in this journal is cited, in accordance with accepted academic practice. No use, distribution or reproduction is permitted which does not comply with these terms.